

# UCSF

## UC San Francisco Previously Published Works

### Title

cAMP Stimulates SLC26A3 Activity in Human Colon by a CFTR-Dependent Mechanism That Does Not Require CFTR Activity.

### Permalink

<https://escholarship.org/uc/item/958926zk>

### Journal

Cellular and molecular gastroenterology and hepatology, 7(3)

### ISSN

2352-345X

### Authors

Tse, Chung-Ming  
Yin, Jianyi  
Singh, Varsha  
et al.

### Publication Date

2019

### DOI

10.1016/j.jcmgh.2019.01.002

Peer reviewed

## ORIGINAL RESEARCH

## cAMP Stimulates SLC26A3 Activity in Human Colon by a CFTR-Dependent Mechanism That Does Not Require CFTR Activity

Chung-Ming Tse,<sup>1,\*</sup> Jianyi Yin,<sup>1,\*</sup> Varsha Singh,<sup>1</sup> Rafiquel Sarker,<sup>1</sup> Ruxian Lin,<sup>1</sup> Alan S. Verkman,<sup>2</sup> Jerrold R. Turner,<sup>3</sup> and Mark Donowitz<sup>1,4</sup><sup>1</sup>Department of Medicine, Division of Gastroenterology and Hepatology, <sup>4</sup>Department of Physiology, Johns Hopkins University School of Medicine, Baltimore, Maryland; <sup>2</sup>Department of Medicine, Department of Physiology, University of California San Francisco, San Francisco, California; <sup>3</sup>Department of Pathology, Department of Medicine, Brigham and Women's Hospital, Harvard Medical School, Boston, Massachusetts

## SUMMARY

New tools (specific antibodies/inhibitor, CRISPR/Cas9 (clustered regularly interspaced short palindromic repeats/Cas9) knock-out, improved functional assay) allowed re-evaluation of 3',5'-cyclicadenosine monophosphate (cAMP) regulation of SLC26A3 down-regulated in adenoma (DRA). cAMP stimulates DRA activity in human embryonic kidney 293 (HEK293)/DRA cells, Caco-2 cells, and human colonoids in a cystic fibrosis transmembrane conductance regulator (CFTR)-dependent manner that does not require CFTR transport activity.

**BACKGROUND & AIMS:** SLC26A3 (DRA) is an electroneutral Cl<sup>-</sup>/HCO<sub>3</sub><sup>-</sup> exchanger that is present in the apical domain of multiple intestinal segments. An area that has continued to be poorly understood is related to DRA regulation in acute adenosine 3',5'-cyclic monophosphate (cAMP)-related diarrheas, in which DRA appears to be both inhibited as part of NaCl absorption and stimulated to contribute to increased HCO<sub>3</sub><sup>-</sup> secretion. Different cell models expressing DRA have shown that cAMP inhibits, stimulates, or does not affect its activity.

**METHODS:** This study re-evaluated cAMP regulation of DRA using new tools, including a successful knockout cell model, a specific DRA inhibitor (DRA<sub>inh</sub>-A250), specific antibodies, and a transport assay that did not rely on nonspecific inhibitors. The studies compared DRA regulation in colonoids made from normal human colon with regulation in the colon cancer cell line, Caco-2.

**RESULTS:** DRA is an apical protein in human proximal colon, differentiated colonoid monolayers, and Caco-2 cells. It is glycosylated and appears as 2 bands. cAMP (forskolin) acutely stimulated DRA activity in human colonoids and Caco-2 cells. In these cells, DRA is the predominant apical Cl<sup>-</sup>/HCO<sub>3</sub><sup>-</sup> exchanger and is inhibited by DRA<sub>inh</sub>-A250 with a median inhibitory concentration of 0.5 and 0.2 μmol/L, respectively. However, there was no effect of cAMP in HEK293/DRA cells that lacked a cystic fibrosis transmembrane conductance regulator (CFTR). When CFTR was expressed in HEK293/DRA cells, cAMP also stimulated DRA activity. In all cases, cAMP stimulation of DRA was not inhibited by CFTR<sub>inh</sub>-172.

**CONCLUSIONS:** DRA is acutely stimulated by cAMP by a process that is CFTR-dependent, but appears to be one of multiple regulatory effects of CFTR that does not require CFTR activity. (*Cell Mol Gastroenterol Hepatol* 2019;7:641–653; <https://doi.org/10.1016/j.jcmgh.2019.01.002>)

**Keywords:** Cl<sup>-</sup>/HCO<sub>3</sub><sup>-</sup> Exchange; CFTR; Colon; Secretory Diarrhea; Enteroids.

There is a long-standing unexplained aspect of the regulation of intestinal electrolyte transport with relevance to the pathophysiology of diarrhea. This relates to acute regulation of SLC26A3 down-regulated in adenoma (DRA) activity. It has been established that DRA is a Cl<sup>-</sup>/HCO<sub>3</sub><sup>-</sup> exchanger that takes part in both intestinal Cl<sup>-</sup> absorption and HCO<sub>3</sub><sup>-</sup> secretion. DRA is expressed differentially along the human intestinal horizontal axis, with maximum expression in the colon > ileum > duodenum >> jejunum. This is consistent with the role for DRA in ileal and proximal colonic neutral NaCl absorption, in which it is linked to Na<sup>+</sup>/H<sup>+</sup> exchanger 3 (NHE3) and performs Cl<sup>-</sup> absorption. DRA also is part of the anion secretory process, accounting for a component of adenosine 3',5'-cyclic monophosphate (cAMP)-stimulated intestinal HCO<sub>3</sub><sup>-</sup> secretion.<sup>1–4</sup>

In cAMP/cholera toxin-related diarrheas, there is both inhibition of neutral NaCl absorption and stimulation of Cl<sup>-</sup> and HCO<sub>3</sub><sup>-</sup> secretion.<sup>5–8</sup> It has never been explained how DRA can be both inhibited and stimulated at the same time

\*Authors share co-first authorship.

**Abbreviations used in this paper:** cAMP, 3',5'-cyclicadenosine monophosphate; CFTR, cystic fibrosis transmembrane conductance regulator; CRISPR/Cas9, clustered regularly interspaced short palindromic repeats/Cas9; DRA, down-regulated in adenoma; IC<sub>50</sub>, median inhibitory concentration; KO, knockout; NHE, Na<sup>+</sup>/H<sup>+</sup> exchanger; pH<sub>i</sub>, intracellular pH.



Most current article

© 2019 The Authors. Published by Elsevier Inc. on behalf of the AGA Institute. This is an open access article under the CC BY-NC-ND license (<http://creativecommons.org/licenses/by-nc-nd/4.0/>).  
2352-345X

<https://doi.org/10.1016/j.jcmgh.2019.01.002>

in cAMP-related diarrhea. Attempts to study cAMP effects on DRA activity in cell-based systems have not been able to answer this question and reported cAMP regulation of DRA is contradictory based on the cell type studied. In HEK293/DRA cells and oocytes, there was no cAMP effect unless the cystic fibrosis transmembrane conductance regulator (CFTR) also was expressed, which led to modest stimulation.<sup>9,10</sup> In Caco-2 cells, cAMP inhibited DRA activity using <sup>36</sup>Cl to measure unidirectional fluxes, which was accompanied by less brush-border DRA.<sup>11</sup> In murine duodenal brush-border vesicle studies, cAMP increased Cl<sup>-</sup>/HCO<sub>3</sub><sup>-</sup> exchange.<sup>12</sup> Most insights concerning basal and cAMP regulation of DRA have come from in vivo mouse studies. Under basal conditions, when NHE3 is present and active, DRA performs net Cl<sup>-</sup> absorption and some HCO<sub>3</sub><sup>-</sup> secretion, whereas if NHE3 is absent or inhibited, DRA performs increased HCO<sub>3</sub><sup>-</sup> secretion but only if CFTR is present.<sup>2,13,14</sup> DRA-mediated HCO<sub>3</sub><sup>-</sup> secretion was stimulated by cAMP in mouse duodenum and colon,<sup>3,4</sup> and the residual HCO<sub>3</sub><sup>-</sup> secretion in DRA-knockout (KO) mice was not sensitive to cAMP.<sup>4</sup> A major gap relevant to understanding human diarrheal disease pathophysiology is that these questions have not been asked in normal human intestine, specifically in the intestinal segments in which most linked NaCl absorption occurs: the ileum and proximal colon.<sup>15,16</sup> Understanding how DRA is regulated by cAMP is especially important because intestinal HCO<sub>3</sub><sup>-</sup> is lost in severe diarrheas, and despite inclusion of HCO<sub>3</sub><sup>-</sup>/citrate in World Health Organization oral rehydration salts solution, the acidosis of severe diarrheas often is inadequately corrected.

Because of the recent availability of multiple new and underused cell systems and specific tools for understanding DRA regulation, we have re-examined the acute effect of cAMP on DRA activity using normal human colonoids, in comparison with the widely used polarized human colon cancer cell line, Caco-2 cells. Colonoids are an ex vivo, self-perpetuating, primary cultured normal human colonic stem cell-derived model that can be grown as monolayers and studied in either an undifferentiated or crypt-like state or a differentiated or surface-like state.<sup>17</sup> Colonoid monolayers from normal human proximal colon were studied because this is a segment in which significant amounts of neutral NaCl absorption occurs along with anion secretion.

## Results

### *DRA Is Expressed in Caco-2 Cells, Proximal Colonoids, and Human Proximal Colon With Increased Expression With Differentiation*

DRA was identified with a commercially available antibody in polarized Caco-2 cells grown on Transwell inserts as a protein with 2 bands: one band of >102 kilodaltons and one band of >76 kilodaltons (Figure 1A), as previously reported.<sup>18</sup> The specificity of this antibody was supported by clustered regularly interspaced short palindromic repeats/Cas9 (CRISPR/Cas9) KO in Caco-2 cells (Figure 1A and B). In addition, although HEK293 cells do not express DRA endogenously, transfection of human DRA showed the same 2 bands.<sup>18</sup> In addition, we previously reported that

deglycosylation of DRA by Peptide:N-glycosidase F (PNGase F) in HEK293/DRA cells and differentiated duodenal enteroids caused both DRA bands to decrease to a common molecular weight just below 76 kilodaltons.<sup>18</sup> Furthermore, DRA expression increases with differentiation, as illustrated in Caco-2 cells grown on semipermeable supports. This is shown in Figure 1C, with a lack of significant DRA expression 4 days after confluency, with increasing expression until days 14 to 18.

In human proximal colonoids, DRA expression also greatly increased in differentiated cells (5 days after wingless-related integration site 3A [WNT3A] removal) compared with undifferentiated cells (grown in the presence of WNT3A) (Figure 1D). This occurred at least in part transcriptionally, as we previously reported, with an increase in DRA messenger RNA of 21-fold upon differentiation of duodenal enteroids determined by quantitative reverse-transcription polymerase chain reaction.<sup>18</sup> In addition, differentiated proximal colonoids had apical and subapical DRA expression, which was much greater than the expression in undifferentiated proximal colonoids (not shown) (Figure 1E).

The increased DRA expression in differentiated proximal colonoids modeled the expression in normal human colon. Immunofluorescence of the normal human proximal colon showed increased DRA expression in the colonic surface and upper crypt compared with the lower crypt (Figure 1F).

### *Cl<sup>-</sup>/HCO<sub>3</sub><sup>-</sup> Exchange Activity in Proximal Colonoids and Caco-2 Cells Is Predominantly via SLC26A3 (DRA) and Not SLC26A6 Putative Anion Transporter-1*

DRA activity was quantified as extracellular Cl<sup>-</sup> removal-driven alkalization in the presence of 25 mmol/L HCO<sub>3</sub><sup>-</sup>/5% CO<sub>2</sub> (Cl<sup>-</sup>/HCO<sub>3</sub><sup>-</sup> exchange) and inhibitors of other acid-base altering transporters, particularly the NHEs. DRA-transfected HEK293 cells showed an immediate initiation of alkalization with removal of extracellular Cl<sup>-</sup> (Figures 2A and D, and 3A), whereas untransfected cells had minimal alkalization (Figure 2D).

Similar rapidly initiated alkalization after apical Cl<sup>-</sup> removal occurred when this assay was applied to Caco-2 cells (21 days after confluency) (Figures 2B and 3B). This alkalization was not present in Caco-2 cells in which DRA was knocked out by CRISPR/Cas9 (Figure 2E). In addition, this alkalization was not affected by the addition of disodium 4,4'-diisothiocyanatostilbene-2,2'-disulfonate (DIDS) (100 μmol/L) to the basolateral side (Figure 2F).

DRA activity also was present and measurable by the apical Cl<sup>-</sup> removal assay in differentiated human colonoid monolayers (Figures 2C and 3C). In all 3 cell types, addition back of Cl<sup>-</sup> to reverse the Cl<sup>-</sup> gradient (apically for Caco-2 and colonoids) rapidly acidified the cells to an intracellular pH (pH<sub>i</sub>) close to the initial pH<sub>i</sub> (Figure 2A–C). In all 3 cell types, multiple cycles of removing and adding Cl<sup>-</sup> back were performed and at least 2 and usually 3 cycles of Cl<sup>-</sup> removal/re-addition led to very similar initial rates of alkalization/acidification (Figure 2A–C). This allowed the use of a single monolayer to determine basal and acutely

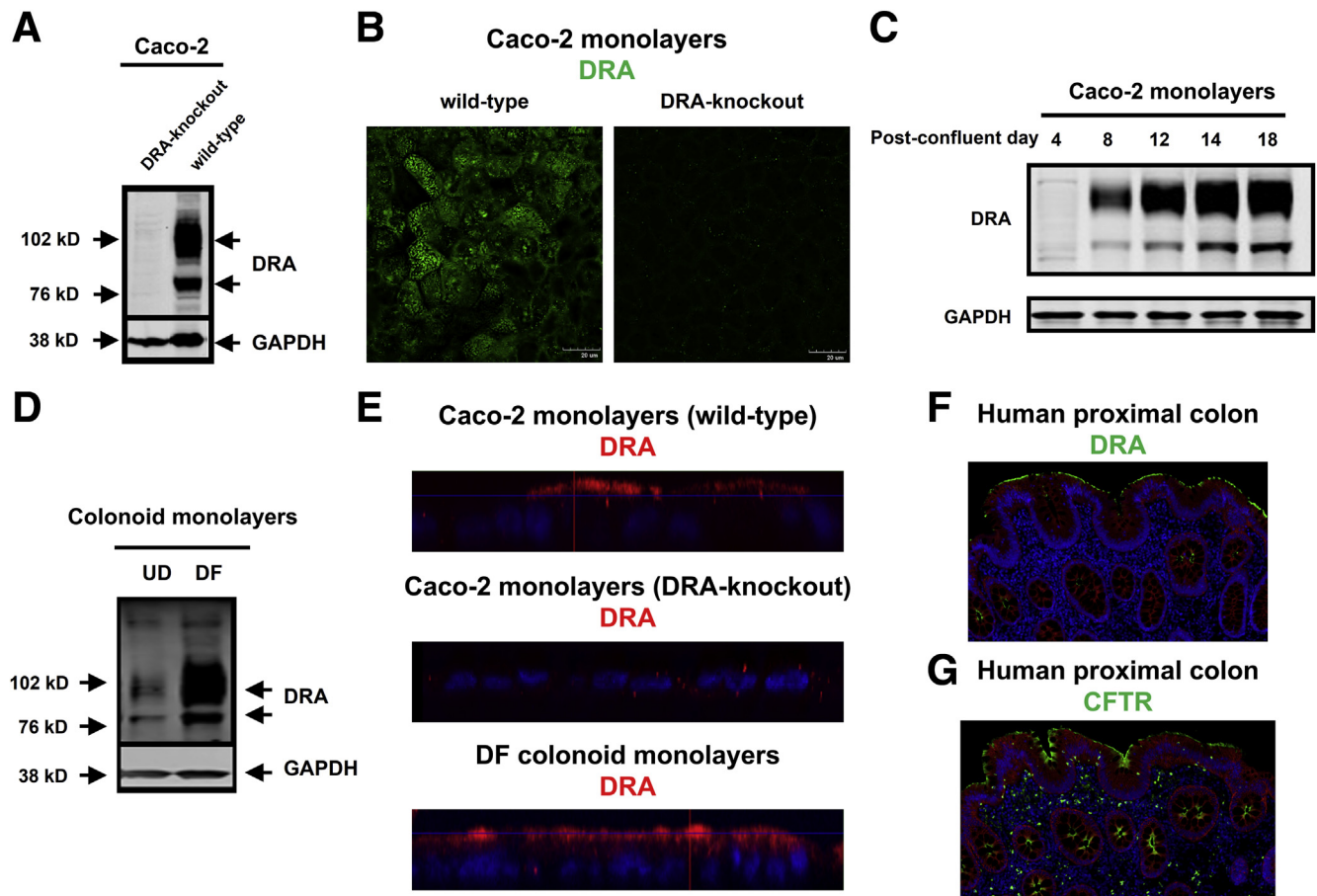


**Figure 1. Protein expression of DRA increases in postconfluent Caco-2 cells and differentiated colonoids.** (A) Immunoblotting of DRA was performed using the mouse monoclonal antibody from Santa Cruz (sc-376187). Two bands of DRA were detected in wild-type Caco-2 cells, whereas no band was identified in DRA-KO Caco-2 cells edited by CRISPR/Cas9. (B) Representative immunofluorescence results showing that DRA protein was detected in wild-type Caco-2 cells but not in DRA-KO Caco-2 cells. (C) In Caco-2 cells that were grown on Transwell inserts, the protein expression of DRA was increased over time after cells reached confluency. (D) Human colonoids were grown on Transwell inserts and differentiated for 5 days. The protein expression of DRA was studied in paired differentiated (DF) and undifferentiated (UD) colonoid monolayers and quantitated using glyceraldehyde-3-phosphate dehydrogenase (GAPDH) as the loading control. DRA protein expression was  $6.8 \pm 1.5$  times higher in differentiated colonoids than undifferentiated colonoids ( $n = 3$ ). (E) Representative immunofluorescence results showing that DRA protein was located mostly on the apical membrane in postconfluent Caco-2 and differentiated colonoid monolayers. Red, DRA; blue, Hoechst. Similar results were seen in 2 repeated experiments. XZ scans are shown including the DRA-KO in Caco-2 cells. (F and G) Representative immunofluorescence results showing the localization of (F) DRA and (G) CFTR in human proximal colon. Images were obtained from the atlas of intestinal transport (<https://www.jrturnerlab.com/Transporter-Images>). Similar results were seen in histologic sections from more than 3 normal subjects for both DRA and CFTR.

regulated DRA activity by studying 2 sequential cycles of apical  $\text{Cl}^-$  removal/re-addition.

Specificity of the assay for DRA activity was established by 2 methods, with the major concern being whether the other SLC26A family member expressed throughout the human gastrointestinal tract, SLC26A6 putative anion transporter-1 (PAT-1), was present and accounted for some or all of the  $\text{Cl}^-$  removal-related alkalinization. The anion, sulfate is transported by PAT-1, but not DRA<sup>19</sup>; thus, whether sulfate could acidify cells when sulfate replaced  $\text{Cl}^-$  in  $\text{Cl}^-$  solution was considered a contribution of PAT-1 and not DRA. As shown in Figure 3 in HEK293/DRA cells, Caco-2 cells, and differentiated colonoids, applying a sulfate

gradient did not acidify  $\text{pH}_i$ , although then adding  $\text{Cl}^-$  (apically for Caco-2 and colonoid monolayers) in the same cells induced rapid intracellular acidification. This finding suggests that these cells showed minimal  $\text{SO}_4^{2-}/\text{HCO}_3^-$  exchange and supports that PAT-1 is not a significant contributor to the  $\text{Cl}^-/\text{HCO}_3^-$  exchange assays in these 3 cell types. In addition, we used a newly described small-molecule DRA inhibitor, DRA<sub>inh</sub>-A250, which lacks effects on other members of the SLC26A family as a second method to determine the specificity of the DRA assay. Inhibition of DRA by DRA<sub>inh</sub>-A250 was reversible, with a median inhibitory concentration ( $\text{IC}_{50}$ ) reported in Fischer rat thyroid (FRT)/DRA cells of approximately  $0.2 \mu\text{mol/L}$ .<sup>20</sup> This



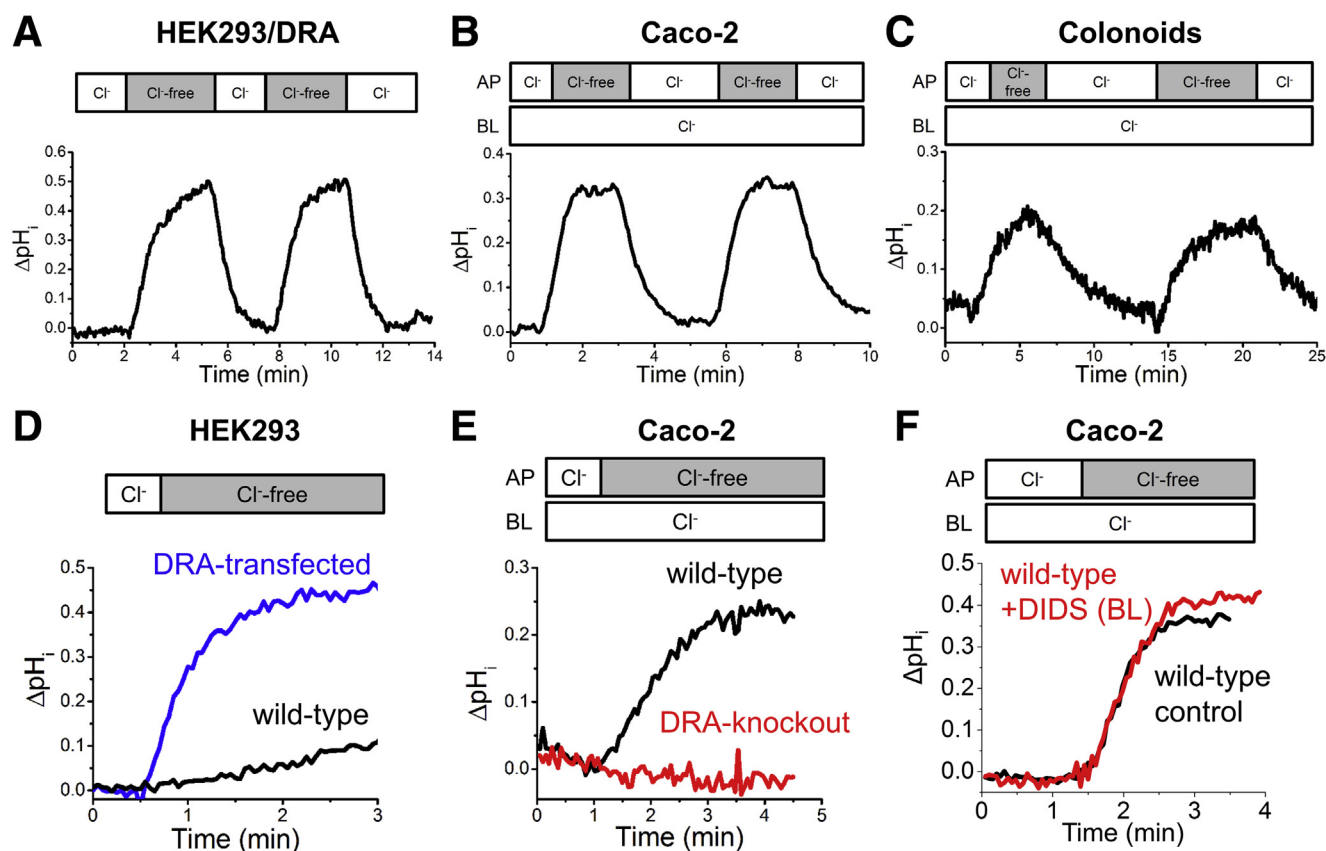


**Figure 2. Validation of  $Cl^-/HCO_3^-$  exchange functional assay.** (A–C)  $Cl^-/HCO_3^-$  exchange activity was determined in (A) HEK293/DRA cells, (B) Caco-2 monolayers, and (C) colonoid monolayers. A rapid intracellular alkalinization was observed after the removal of extracellular  $Cl^-$ , and a rapid intracellular acidification occurred after the replenishment of extracellular  $Cl^-$ . Multiple cycles of removing and replenishing extracellular  $Cl^-$  were performed in a single sample. Compared with the first cycle, the second cycle gave a very similar rate of intracellular alkalinization (HEK293/DRA, 100%  $\pm$  9%, n = 11; Caco-2, 99%  $\pm$  5%, n = 7; colonoids, 103%  $\pm$  4%, n = 13). (D) The initial rate of intracellular alkalinization after extracellular  $Cl^-$  removal was greater in HEK cells expressing DRA (0.63  $\pm$  0.10/min, n = 13) than wild-type HEK cells (0.05  $\pm$  0.01/min, n = 13). The endogenous alkalinization in wild-type HEK cells contributed to only a small percentage (8%) of alkalinization in HEK293/DRA cells. (E) Postconfluent Caco-2 cells showed endogenous  $Cl^-/HCO_3^-$  exchange activity, whereas DRA-knockout Caco-2 cells had no detectable  $Cl^-/HCO_3^-$  exchange activity. n = 3 for each. (F) The addition of DIDS (100  $\mu$ mol/L) to the basolateral side caused no change in the apical  $Cl^-/HCO_3^-$  exchange activity in Caco-2 cells (92%  $\pm$  12%, n = 3). AP, apical; BL, basolateral.

inhibitor similarly inhibited DRA in HEK293/DRA cells, Caco-2 cells, and human colonoids (Figure 4A–C). In HEK293/DRA cells, Caco-2 cells, and colonoids, the  $IC_{50}$  was determined as 0.12  $\pm$  0.04  $\mu$ mol/L, 0.53  $\pm$  0.10  $\mu$ mol/L, and 0.22  $\pm$  0.08  $\mu$ mol/L, respectively (n = 3 for each). These studies indicated that apical  $Cl^-/HCO_3^-$  exchange activity in HEK293/DRA, Caco-2, and proximal colonoids was almost entirely caused by DRA activity.

### cAMP Rapidly Stimulates DRA by a CFTR-Dependent Process That Does Not Require CFTR Activity

To determine whether cAMP acutely affects DRA activity, studies were performed in HEK293 and Caco-2 cells and in human colonoid monolayers. Initial studies were performed in HEK293 cells that stably express human DRA but do not express CFTR endogenously.<sup>9,21</sup> DRA activity was present

but exposure to forskolin (10  $\mu$ mol/L, 10 min) did not alter DRA activity (Figure 5A and B).

Similar studies were performed in Caco-2 cells and human colonoids. Results were different; as shown in Figure 5C and D, forskolin (10  $\mu$ mol/L, 10 min) caused acute stimulation of DRA activity in both Caco-2 and colonoid monolayers. It was further determined whether cAMP-dependent stimulation of DRA was associated with stimulation of DRA trafficking. This was performed by cell surface biotinylation. Forskolin (10  $\mu$ mol/L, 30 min) significantly increased total DRA cell surface expression (22.5%  $\pm$  4.8%) in Caco-2 cells (Figure 6A and B). The surface-to-total ratio of the higher molecular weight highly glycosylated band showed a significant increase with forskolin (27.6%  $\pm$  3.2%), while the core glycosylated band did not significantly change (4.3%  $\pm$  2.2%). Similar studies of cell surface biotinylation of DRA 10 minutes after forskolin had a slightly, but not significantly, greater increase in total DRA surface

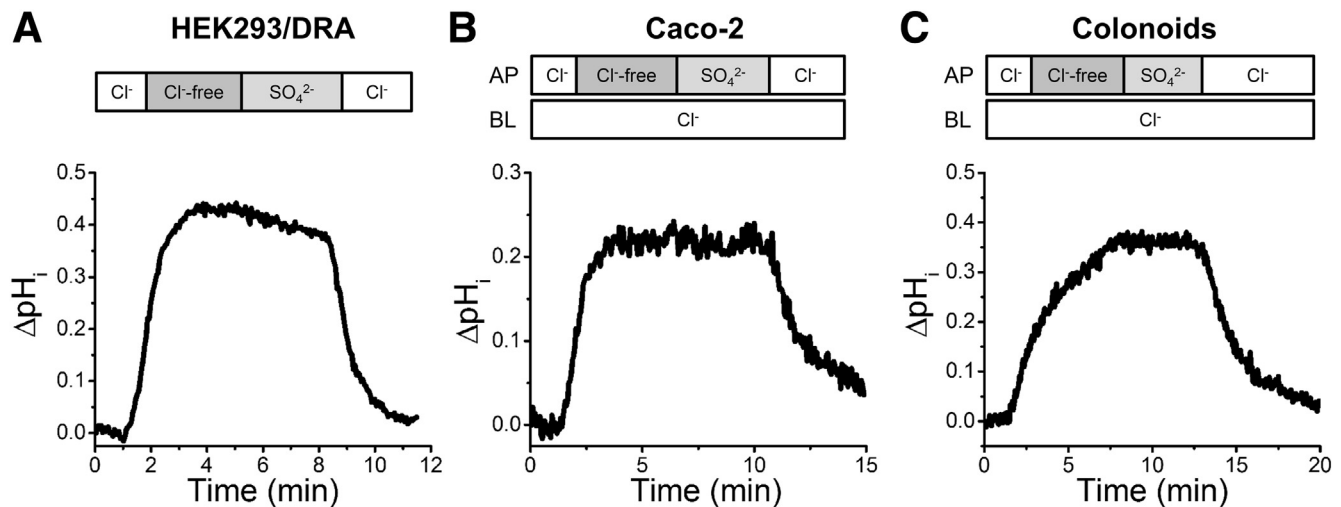


**Figure 3.**  $Cl^-/HCO_3^-$  exchange is performed by an ion transporter that is not able to mediate  $SO_4^{2-}/HCO_3^-$  exchange.  $SO_4^{2-}/HCO_3^-$  exchange activity was studied using a  $SO_4^{2-}$ -based superfusate that does not contain  $Cl^-$ . In these experiments, the NHE3 inhibitor tenapanor (provided by Ardelyx, Inc, Fremont, CA) and the NHE1 and NHE2 inhibitor HOE-694 (provided by Jorgen Peunter, Sanofi) were used in lieu of amiloride in the  $SO_4^{2-}$ -based superfusate. Although  $Cl^-/HCO_3^-$  exchange was observed, no  $SO_4^{2-}/HCO_3^-$  exchange activity was detected in (A) HEK293/DRA cells, (B) Caco-2 monolayers, or (C) colonoid monolayers, suggesting the process of  $Cl^-/HCO_3^-$  exchange in these cell models was performed by an ion transporter that is not able to perform  $SO_4^{2-}/HCO_3^-$  exchange. These experiments were repeated at least 3 times and similar results were found in each experiment. AP, apical; BL, basolateral.

expression ( $36.7\% \pm 7.3\%$ ;  $n = 3$ ). Similar changes in DRA surface expression after forskolin were demonstrated using immunofluorescence in Caco-2 cells (Figure 6C–E). Because the presence of CFTR in oocytes was sufficient for cAMP stimulation in DRA activity to occur,<sup>10</sup> it was determined whether forskolin stimulated DRA activity in HEK293/DRA cells that expressed CFTR. HEK293 cells do not endogenously express CFTR.<sup>21</sup> Lipofectamine transfection was used to transiently express GFP-CFTR and more than 90% of cells expressed GFP-CFTR after transfection as confirmed by microscopic observation using a Keyence BZ-X700 fluorescence microscope (Itasca, IL). Forskolin stimulated DRA

activity in HEK293/DRA cells transfected with CFTR (Figure 7A). CFTR transports  $HCO_3^-$ , with a lower permeability compared with  $Cl^-$ , but there is increasing  $HCO_3^-$  permeability at least in some cell types with intracellular  $Cl^-$  depletion, as initially occurs with cAMP-stimulated  $Cl^-$  secretion.<sup>22</sup> Consequently, we considered whether the CFTR/forskolin-dependent increase in intracellular alkalinization after  $Cl^-$  removal could be owing to CFTR transporting  $HCO_3^-$ . This was examined by studying the forskolin effect on DRA activity in HEK293/DRA/CFTR cells when CFTR activity was inhibited using the CFTR inhibitor CFTR<sub>inh</sub>-172. CFTR<sub>inh</sub>-172 did not alter either the basal DRA

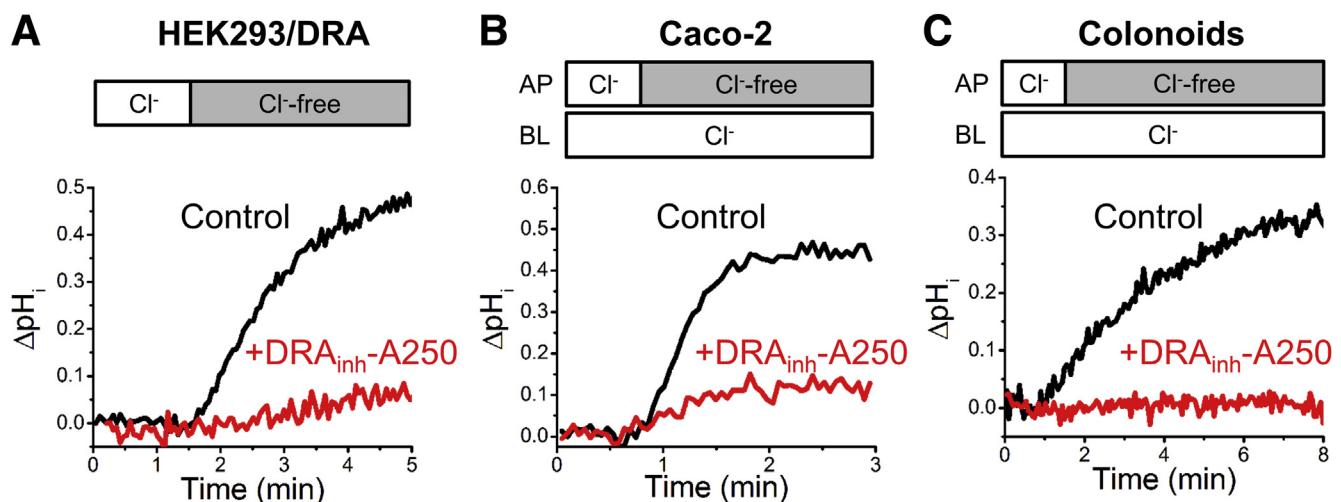


**Figure 4.** Effect of DRA inhibitor on  $Cl^-/HCO_3^-$  exchange. (A–C) The  $Cl^-/HCO_3^-$  exchange activity in (A) HEK293/DRA cells, (B) Caco-2 monolayers, and (C) colonoid monolayers was mostly abolished by a novel DRA inhibitor, DRA<sub>inh</sub>-A250 (5  $\mu$ mol/L, apical and basolateral), indicating that DRA is the major  $Cl^-/HCO_3^-$  exchanger in these 3 cell types. AP, apical; BL, basolateral.

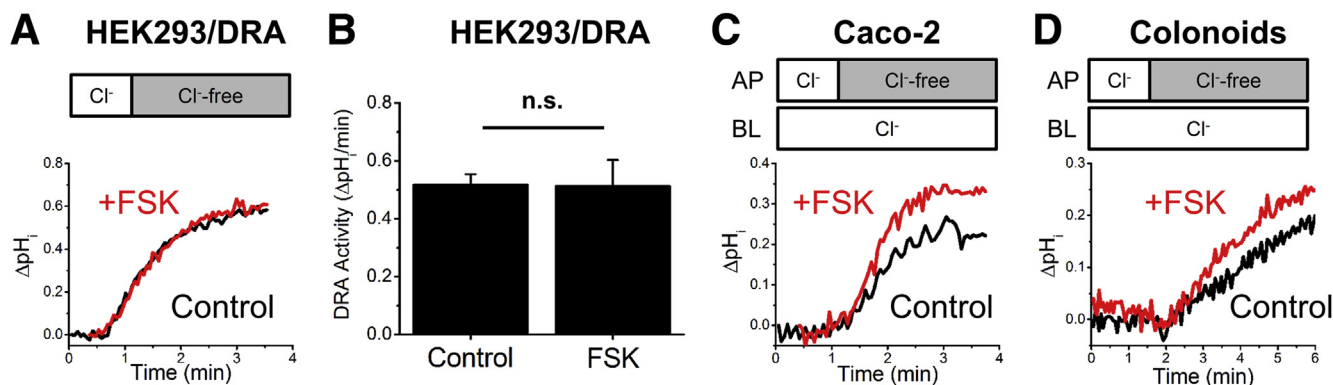


**Figure 5. Forskolin stimulates DRA activity in Caco-2 and human colonoids but not in HEK293/DRA cells.** (A and B) Forskolin (FSK) did not change the DRA activity in HEK293/DRA cells ( $n = 6$ ). (C and D) Representative traces showing that forskolin stimulates DRA activity in (C) Caco-2 monolayers and (D) colonoid monolayers. Quantitation of the change in DRA activity by forskolin in Caco-2 cells and colonoids is shown in Figure 8. AP, apical; BL, basolateral.

activity in HEK293/DRA cells, or the forskolin stimulation of DRA activity in HEK293/DRA/CFTR cells measured as  $\text{Cl}^-$  removal-stimulated alkalinization (Figure 7). This shows that cAMP stimulation of DRA requires CFTR but does not require CFTR transport activity.

Caco-2 cells are known to express CFTR. Similarly, immunofluorescence of differentiated human proximal colonoids showed expression of CFTR as well as DRA in the apical domain (Figure 1F and G). Similar studies to those in HEK cells determined whether CFTR activity was necessary for forskolin stimulation of DRA in Caco-2 cells and human colonoids. Inhibiting CFTR with CFTR<sub>inh</sub>-172 did not affect forskolin stimulation of DRA activity in either Caco-2 cells (Figure 8A–C) or colonoids (Figure 8D–F).

## Discussion

DRA is a glycoprotein, both when exogenously expressed in HEK293 cells and Chinese hamster ovary (CHO) cells or endogenously expressed in mouse intestine.<sup>23–26</sup> Its molecular size as shown by Western blot varies and this is probably owing to heterogenous glycosylation in different cell systems and animal species.<sup>23–27</sup> We report here that human DRA in HEK293/DRA cells, Caco-2 cells, and differentiated proximal colonoids appears as 2 bands: the upper band is slightly higher than 102 kilodaltons and the lower band is slightly higher than 76 kilodaltons, and, as previously shown, both of these bands are glycosylated.<sup>18</sup> The distribution of DRA throughout the human gastrointestinal tract both horizontally and vertically has been described. It is widely believed that DRA functions as a  $\text{Cl}^-/\text{HCO}_3^-$  exchanger with 1:1 stoichiometry,<sup>28</sup> but controversy exists and some results have indicated that its transport in mice is electrogenic and it can function as an uncoupled anion conductance at low  $\text{Cl}^-$ .<sup>9</sup> In addition, there continues to be confusion relating to its acute regulation, particularly in digestive physiology and in the pathophysiology of cAMP-driven secretory diarrheal diseases. The current study was performed to re-evaluate acute regulation of DRA based on the availability of new normal human colonoid models that

are segment-specific, allowing what occurs in the human proximal colon to be examined. The proximal colon was selected for study because it is the site of high DRA expression and is known to be the site of a large amount of  $\text{Na}^+$  absorption, specifically neutral  $\text{NaCl}$  absorption, and also of anion secretion, both processes in which DRA has been implicated. Importantly, the ability to study only epithelial cells in the stem cell-derived colonoids allows better control of transport regulation. In addition, studying differentiated colonoids as monolayers, which represent the upper crypt and surface cells compared with undifferentiated colonoids representing the lower crypt, allowed concentration on the proximal colonic cells with the highest DRA expression with results not diluted by lower-expressing cells. This study also re-evaluated acute regulation of DRA because there are more specific tools than what have been available previously that include a DRA-specific, small-molecule inhibitor (DRA<sub>inh</sub>-A250), and DRA-KO by CRISPR/Cas9, as well as antibody validated by KO and expression in null cells; an assay of DRA activity that does not rely on nonspecific antagonists, such as DIDS or niflumic acid; and, finally, an assay measuring  $\text{Cl}^-/\text{HCO}_3^-$  exchange instead of hydroxide/iodide exchange because hydroxide ion may not be an adequate substrate of DRA.<sup>29</sup>

Emphasis was on DRA regulation by increased cAMP because of the importance of both inhibition of neutral  $\text{NaCl}$  absorption and stimulation of active anion secretion in secretory but noninflammatory diarrheas. Both processes occur in the proximal colon and examples of DRA regulation in diarrhea models in this segment have been reported, including salmonella in which DRA message and protein are reduced, and enteropathogenic *E. coli* (EPEC), in which surface expression is reduced.<sup>30,31</sup> There also have been inconsistent previous reports of cAMP effects on DRA activity in multiple cell models as reviewed in the introduction section of this article, and some segment-specific differences described for mouse intestine. In mouse duodenum, forskolin stimulates  $\text{HCO}_3^-$  secretion by a DRA-dependent process that also requires CFTR including CFTR activity.<sup>2,3</sup> In mid-distal mouse colon, in which a large amount of

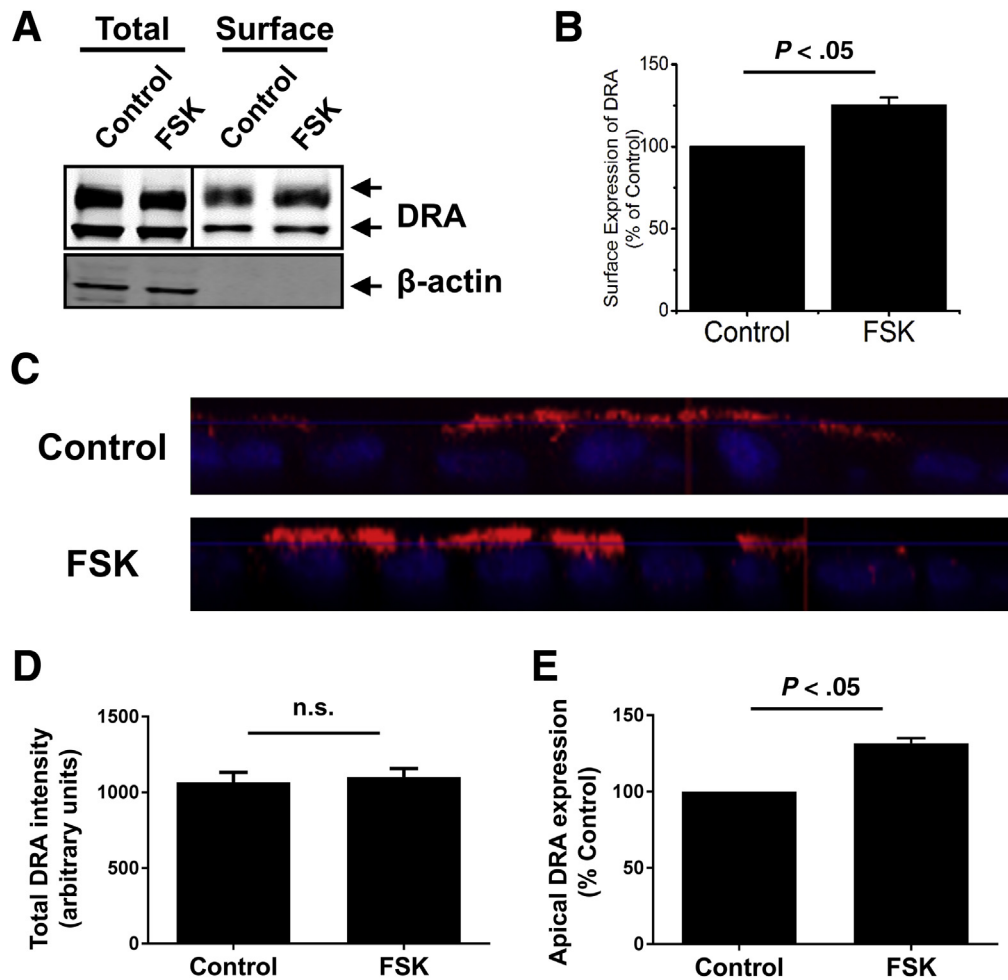


**Figure 6. Forskolin (FSK) increases the surface amount of DRA protein in Caco-2 cells.** (A and B) The surface expression of DRA protein was studied by surface biotinylation. Forskolin (10  $\mu$ mol/L, apical and basolateral, 30 min) caused an increase in the percentage of surface amount without changing the total amount of DRA protein in postconfluent Caco-2 monolayers. Quantitation was performed by comparing forskolin-treated and untreated control samples with controls in each experiment set as 100% ( $n = 4$ ). (C–E) Representative immunofluorescence results showing an increased amount of DRA protein in the apical domain of polarized proximal colonoid cells after forskolin treatment (10  $\mu$ mol/L, apical and basolateral, 10 min). Each panel shows XZ projection. Quantification of the DRA intensity in control and forskolin-treated monolayers was performed with Volocity Software (PerkinElmer, Waltham, MA). (D) The total DRA amount was not increased with forskolin treatment. Quantification of the percentage of apical DRA in the juxta-apical region (stacks 1–3, each stack 1- $\mu$ m XZ dimension, 20–25  $\mu$ m total cell height) was normalized to total DRA (whole image) expression set as 100% for each experiment. At least 3 separate images and 4 random individual areas (Z sections) were analyzed for each group. Scale bar: 10  $\mu$ m. Results are means  $\pm$  SEM.  $P$  values are a comparison with the untreated control ( $n = 3$ ).

DRA is expressed, basal  $\text{HCO}_3^-$  secretion was DRA-dependent but CFTR-independent; however, with forskolin stimulation, the increased  $\text{HCO}_3^-$  secretion was dependent on CFTR.<sup>32</sup>

The finding presented here is that in both Caco-2 cells and human proximal colonic enteroids, forskolin stimulates DRA activity by a CFTR-dependent process, which is similar to what occurs in the mouse duodenum and mid-distal colon.<sup>3,4</sup> Forskolin/cAMP did not directly activate DRA because its stimulatory effect occurred in HEK293/DRA/CFTR cells, but not HEK293/DRA cells. In addition, CFTR<sub>inh</sub>-172 had no effect on forskolin stimulation of DRA activity, suggesting that the increased rate of intracellular alkalinization in the presence of forskolin was not due to

direct secretion of  $\text{HCO}_3^-$  via CFTR in our assay. This represents another example of the regulatory function of CFTR that does not require the transport function of CFTR.<sup>33</sup> The current study concentrated only on human proximal colonoids that were differentiated and thus represented surface and upper crypt epithelial cells. Similarly, we showed by immunofluorescence that intact normal human proximal colon upper crypt and surface epithelial cells contained both CFTR and DRA. Moreover, the forskolin stimulation was associated with increased surface DRA, supporting the involvement of trafficking or increased plasma membrane stability in the mechanism of the cAMP stimulation of DRA. However, the fact that cAMP stimulated DRA activity with a higher percentage increase than it increased surface DRA



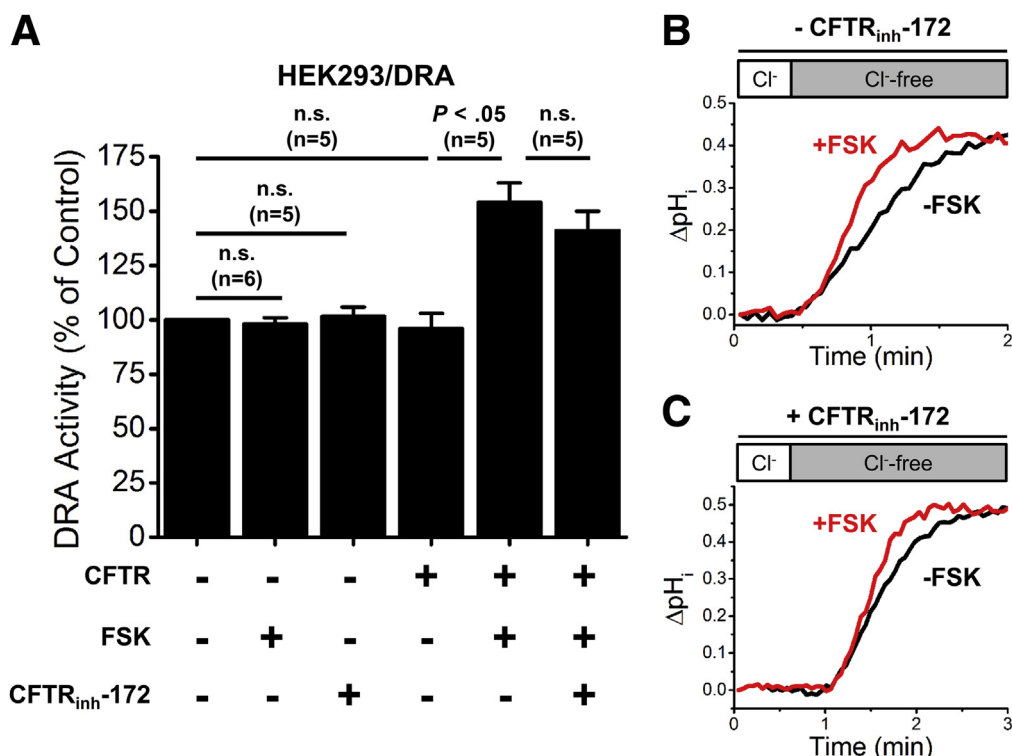


**Figure 7.** Expression of CFTR in HEK293/DRA cells reconstitutes the stimulatory effect of forskolin (FSK) on DRA activity, which is independent of CFTR function. (A) DRA activity was determined in HEK293/DRA cells as well as HEK293/DRA cells that were transiently transfected with CFTR, using superfusate that contained forskolin (10  $\mu$ mol/L) and/or CFTR<sub>inh</sub>-172 (5  $\mu$ mol/L). Data were normalized to that of HEK293/DRA cells under basal condition (set as 100%). A stimulatory effect of forskolin on DRA activity was observed in CFTR-expressing cells, and the stimulation was not affected by inhibiting CFTR activity using CFTR<sub>inh</sub>-172. The number of experiments is shown as n. P values are shown for the specific comparisons designated. (B and C) Representative traces showing the stimulatory effect of forskolin on DRA activity in HEK293/DRA/CFTR cells, in the (B) absence and the (C) presence of CFTR<sub>inh</sub>-172.

expression suggests that this involves regulation in addition to changes in trafficking; even considering that only the higher molecular weight band was involved in increased surface expression and transport activity.

Intestine is not the only transporting tissue that expresses CFTR and Cl<sup>-</sup>/HCO<sub>3</sub><sup>-</sup> exchangers of the SLC26A family. Studies in the widely studied human airway cell line Calu-3 examined mechanisms of cAMP-stimulated HCO<sub>3</sub><sup>-</sup> secretion.<sup>34</sup> These cells express a large amount of CFTR and much less SLC26A4 (pendrin). As reported, forskolin-stimulated HCO<sub>3</sub><sup>-</sup> secretion in Calu-3 cells was entirely CFTR-dependent and not affected by SLC26A4 knockdown, identifying an additional model of cAMP-stimulated HCO<sub>3</sub><sup>-</sup> secretion in cells that contain both CFTR and members of the SLC26 family.<sup>34</sup> Of note, pendrin contributed to the forskolin-stimulated HCO<sub>3</sub><sup>-</sup> secretion in another Calu-3 study.<sup>35</sup>

The mechanism by which CFTR is necessary for cAMP stimulation of DRA activity has not been determined in human intestinal epithelial cells, including proximal colonoids. However, Ko et al<sup>35</sup> used nonpolarized HEK293 cells expressing CFTR and DRA to suggest a mechanism that involved mutual activation of DRA and CFTR. They showed in oocytes that CFTR and DRA were in the same complex (based on coprecipitation), and forskolin-stimulated HCO<sub>3</sub><sup>-</sup>

secretion required DRA activity and was not accounted for by CFTR transporting HCO<sub>3</sub><sup>-</sup>.<sup>35</sup> cAMP caused DRA and CFTR to mutually activate each other by a mechanism that required the presence of both their C-terminal PDZ domain interaction sequences and involved the cAMP phosphorylated CFTR R domain and the DRA sulfate transporter and anti-sigma factor antagonist (STAS) domain. This activation of CFTR was not the result of alteration of cAMP stimulation of its trafficking. Although DRA activity was not explicitly shown to be required for CFTR activation, mutated DRA found in congenital Cl<sup>-</sup> diarrhea did not allow the cAMP activation of CFTR. Although this has not yet been evaluated in human proximal colonoids, we hypothesize that the cAMP stimulation of DRA activity requiring CFTR but not CFTR transport activity in polarized human intestinal cells is likely to occur by a mechanism(s) similar to the interactions shown by Ko et al.<sup>35</sup>

Our study shows in HEK293/DRA cells, Caco-2 cells, and human colonoids that forskolin stimulation of DRA is CFTR-dependent but that dependence does not require CFTR transport activity. This cAMP stimulation of DRA activity in human proximal colonoids and Caco-2 cells occurs by a process that requires CFTR, separate from CFTR transport activity and different from the interactions identified in

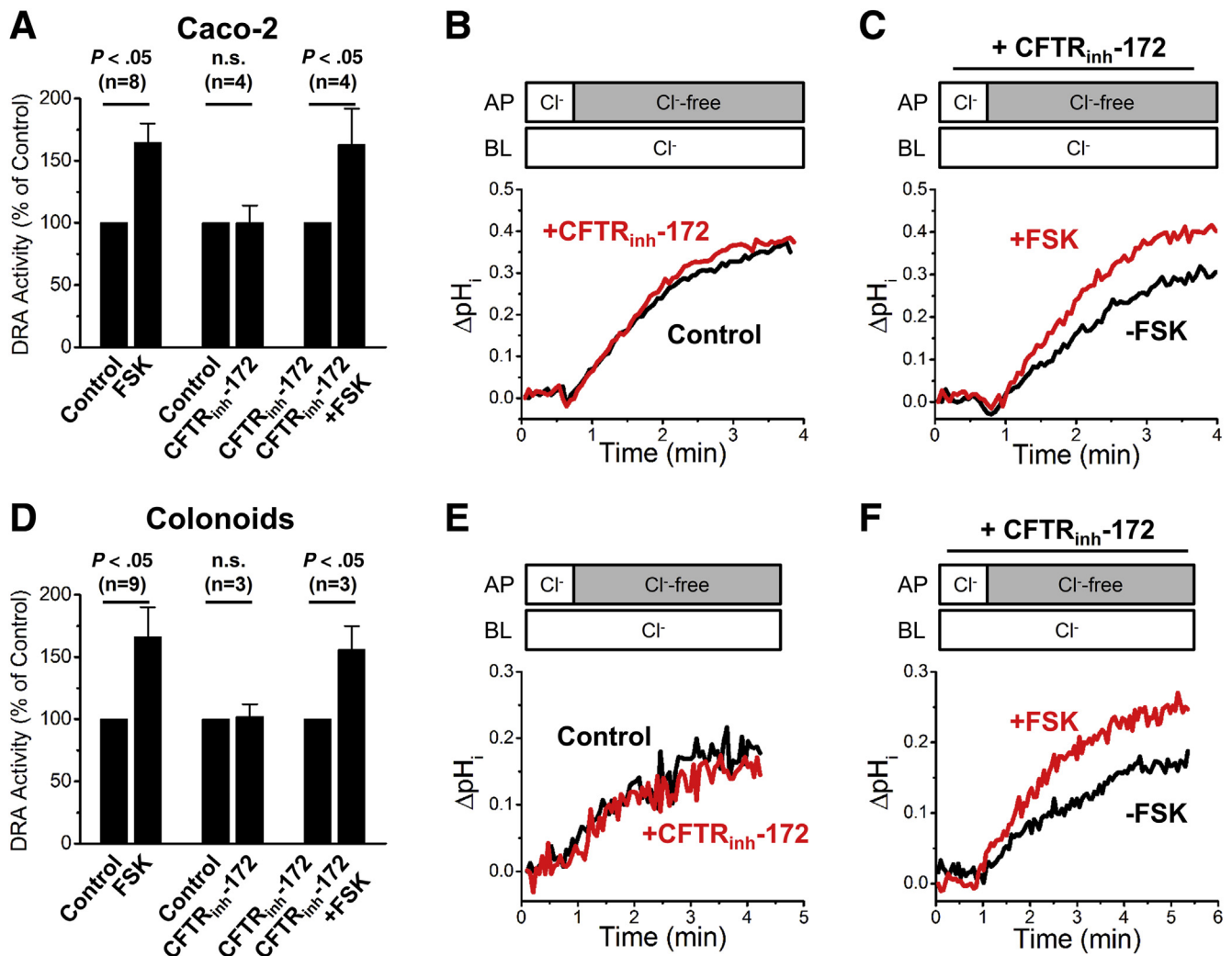


**Figure 8.** CFTR<sub>inh</sub>-172 does not affect the stimulatory effect of forskolin on DRA activity in Caco-2 and colonoid monolayers. In (A–C) Caco-2 monolayers and (D–F) colonoid monolayers, CFTR<sub>inh</sub>-172 did not change the (B and E) basal activity of DRA or the (C and F) stimulatory effect of forskolin. The number of experiments is shown as n. P values are shown for the specific comparisons designated. AP, apical; BL, basolateral.

several other transporting epithelial cells, with multiple pathophysiologic mechanisms having evolved for cAMP-related HCO<sub>3</sub><sup>-</sup> secretion in polarized epithelia. Those reported vary from HCO<sub>3</sub><sup>-</sup> secretion entirely via CFTR (Calu-3 cells) to involving DRA and requiring CFTR protein and transport activity (mouse duodenum and mid-distal colon). HCO<sub>3</sub><sup>-</sup> secretion functions to unfold mucus including that secreted by goblet cells, which is protective against pathogens and inhaled physical agents. From an evolutionary perspective, HCO<sub>3</sub><sup>-</sup> secretion has important protective functions in multiple tissues and thus it is not unexpected that the multiple mechanisms that regulate HCO<sub>3</sub><sup>-</sup> secretion have evolved.

## Materials and Methods

Chemicals and reagents were purchased from Thermo Fisher (Waltham, MA) or Sigma-Aldrich (St. Louis, MO)

unless otherwise specified. All authors had access to the study data and reviewed and approved the final manuscript.

## Cell Culture

HEK293 cells were cultured in Dulbecco's modified Eagle medium/nutrient mixture F-12 supplemented with 10% fetal bovine serum, 100 U/mL penicillin, and 100 μg/mL streptomycin in a 5% CO<sub>2</sub>/95% air atmosphere at 37°C. The plasmid pCMV-SPORT6-SLC26A3 (human) was purchased from the DNA Resource Core at Harvard Medical School (Boston, MA). p3xFLAG-DRA was constructed by inserting human SLC26A3 into p3xFLAG-CMV-10 between XbaI and BamHI. A stable cell line that expresses p3xFLAG-DRA was established using Lipofectamine 2000 according to the manufacturer's protocol and selected by G418 exposure. In some experiments, cells were transfected with N-terminal green fluorescent protein (GFP)-CFTR (provided by Dr

Liudmila Cebotaru, Johns Hopkins University) and studied at 48–72 hours after transfection.

Caco-2 cells were cultured in Dulbecco's modified Eagle medium supplemented with 25 mmol/L NaHCO<sub>3</sub>, 0.1 mmol/L nonessential amino acids, 10% fetal bovine serum, 4 mmol/L glutamine, 100 U/mL penicillin, and 100 µg/mL streptomycin in a 5% CO<sub>2</sub>/95% air atmosphere at 37°C. To generate a DRA-KO Caco-2 cell line, cells were transduced with a lentivirus expressing doxycycline-inducible Cas9 followed by a lentivirus expressing a specific green fluorescent protein (sgRNA) that targets human DRA (GGACTGGGTAACATAGTCTG, NCBI reference sequence: NM\_000111.2). After induction by doxycycline and selection by puromycin/blasticidin exposure, positive clones were identified by immunoblotting. Genomic DNA was extracted, the target regions were amplified by polymerase chain reaction, and sequenced by Sanger sequencing (MacroGen, Rockville, MD). For experiments, cells were plated on Transwell inserts (Corning, Inc, Corning, NY) and studied at 14–18 days after reaching confluency.

Endoscopic specimens of human proximal colon from healthy human subjects were used to establish primary cultures of human colonoids as previously described.<sup>17,36</sup> Colonoids were expanded and plated on Transwell inserts (Corning, Inc) to form monolayers, as previously described.<sup>17,18</sup> For differentiation, colonoids were maintained in a medium that lacked WNT3A, R-spondin1, and SB202190 for 5 days.<sup>18</sup> Most results of the current study were obtained from colonoids derived from 1 healthy donor, with similar results observed in colonoids from 2 other donors. The procurement and study of human colonoids was approved by the Institutional Review Board of Johns Hopkins University School of Medicine (NA\_00038329).

### Immunofluorescence

Cells were fixed in 4% paraformaldehyde for 20 minutes, incubated with 5% bovine serum albumin/0.1% saponin in phosphate-buffered saline for 1 hour, and incubated with primary antibody against DRA (mouse monoclonal, 1:100, sc-376187; Santa Cruz, Dallas, TX) overnight at 4°C. Cells then were incubated with Hoechst 33342 and secondary antibody against mouse IgG (1:100) for 1 hour at room temperature. Finally, cells were mounted and studied using a Carl Zeiss LSM510/META confocal microscope (Thornwood, NY). In addition, the atlas of intestinal transport (<https://www.jrturnerlab.com/Transporter-Images>) was accessed to determine the localization of DRA and CFTR in healthy human proximal colon.

### Immunoblotting

Cells were rinsed 3 times with phosphate-buffered saline and harvested in phosphate-buffered saline by scraping. Cell pellets were collected by centrifugation, solubilized in lysis buffer (60 mmol/L HEPES, 150 mmol/L NaCl, 3 mmol/L KCl, 5 mmol/L EDTA trisodium, 3 mmol/L ethylene glycol-bis(β-aminoethyl ether)-N,N,N',N'-tetraacetic acid,

1 mmol/L Na<sub>3</sub>PO<sub>4</sub>, and 1% Triton X-100, pH 7.4) containing a protease inhibitor cocktail, and homogenized by sonication. Protein concentration was measured using the bicinchoninic acid method. Proteins were incubated with sodium dodecyl sulfate buffer (5 mmol/L Tris-HCl, 1% sodium dodecyl sulfate, 10% glycerol, 1% 2-mercaptoethanol, pH 6.8) at 37°C for 10 minutes, separated by sodium dodecyl sulfate–polyacrylamide gel electrophoresis on a 10% acrylamide gel, and transferred onto a nitrocellulose membrane. The blot was blocked with 5% nonfat milk, probed with primary antibodies against DRA (mouse monoclonal, 1:500, sc-376187; Santa Cruz), glyceraldehyde-3-phosphate dehydrogenase (mouse monoclonal, 1:5000, G8795; Sigma-Aldrich), β-actin (mouse monoclonal, 1:5000, A2228; Sigma-Aldrich) overnight at 4°C, followed by secondary antibody against mouse IgG (1:10,000) for 1 hour at room temperature. Protein bands were visualized and quantitated using an Odyssey system and Image Studio software (LI-COR Biosciences, Lincoln, NE).

### Surface Biotinylation

At 4°C, cells were incubated with 1.5 mg/mL N-hydroxysulfosuccinimide (NHS)-SS-biotin N-Hydroxysulfosuccinimide- and solubilized by lysis buffer. A small proportion of the protein lysate was collected as the total lysate, while the rest was incubated with avidin-agarose beads overnight. The beads were centrifuged and washed with lysis buffer containing 0.1% Triton X-100. Biotinylated proteins were eluted from the beads and collected as the surface fraction. Immunoblotting was performed as described earlier and the percentage of surface expression of DRA was calculated as previously reported by loading equal volumes for each total and surface fraction.<sup>37</sup> The surface to total ratio was calculated separately for the upper band (highly glycosylated, ~102 kilodaltons in size), the lower band (core glycosylated, ~85 kilodaltons in size), as well as for both bands together.

### Measurement of Cl<sup>-</sup>/HCO<sub>3</sub><sup>-</sup> Exchange Activity

Cl<sup>-</sup>/HCO<sub>3</sub><sup>-</sup> exchange activity was measured fluorometrically using the pH<sub>i</sub>-sensitive dye BCECF-AM and a custom chamber allowing separate apical and basolateral superfusion, as previously described.<sup>38</sup> Cells were incubated with 10 µmol/L BCECF-AM in Na<sup>+</sup> solution (138 mmol/L NaCl, 5 mmol/L KCl, 2 mmol/L CaCl<sub>2</sub>, 1 mmol/L MgSO<sub>4</sub>, 1 mmol/L NaH<sub>2</sub>PO<sub>4</sub>, 10 mmol/L glucose, 20 mmol/L HEPES, pH 7.4) for 30–60 minutes at 37°C and mounted in a fluorometer (Photon Technology International, Birmingham, NJ). Cells were superfused with Cl<sup>-</sup> solution (110 mmol/L NaCl, 5 mmol/L KCl, 1 mmol/L CaCl<sub>2</sub>, 1 mmol/L MgSO<sub>4</sub>, 10 mmol/L glucose, 25 mmol/L NaHCO<sub>3</sub>, 1 mmol/L amiloride, 5 mmol/L HEPES, 95% O<sub>2</sub>/5% CO<sub>2</sub>) or Cl<sup>-</sup>-free solution (110 mmol/L Na-gluconate, 5 mmol/L K-gluconate, 5 mmol/L Ca-gluconate, 1 mmol/L Mg-gluconate, 10 mmol/L glucose, 25 mmol/L NaHCO<sub>3</sub>, 1 mmol/L amiloride, 5 mmol/L HEPES, 95% O<sub>2</sub>/5% CO<sub>2</sub>) under a flow rate of 1 mL/min. The switch between Cl<sup>-</sup> solution and

Cl<sup>-</sup>-free solution causes HCO<sub>3</sub><sup>-</sup> movement across the cell membrane performed by Cl<sup>-</sup>/HCO<sub>3</sub><sup>-</sup> exchanger(s), and the resulting change in pH<sub>i</sub> was recorded. For Caco-2 and colonoid monolayers, the apical side was superfused with Cl<sup>-</sup> solution or Cl<sup>-</sup>-free solution, while the basolateral side was superfused continuously with Cl<sup>-</sup> solution. Multiple rounds of removing/replenishing extracellular Cl<sup>-</sup> were performed to determine the Cl<sup>-</sup>/HCO<sub>3</sub><sup>-</sup> exchange activity under basal conditions as a time control as well as in the presence of several compounds, including forskolin (10 μmol/L, apical and basolateral) and CFTR<sub>inh</sub>-172 (5 μmol/L, apical). The cells were exposed to these compounds for at least 8 minutes before their effects on Cl<sup>-</sup>/HCO<sub>3</sub><sup>-</sup> exchange activity was determined. In some experiments, SO<sub>4</sub><sup>2-</sup> solution (55 mmol/L Na<sub>2</sub>SO<sub>4</sub>, 55 mmol/L mannitol, 5 mmol/L K-gluconate, 1 mmol/L Ca-gluconate, 1 mmol/L Mg-gluconate, 10 mmol/L glucose, 25 mmol/L NaHCO<sub>3</sub>, 2 μmol/L Tenapanor [provided by Ardelyx, Inc, Fremont, CA], 10 μmol/L HOE-694 [provided by Jorgen Peunter, Sanofi], 5 mmol/L HEPES, 95% O<sub>2</sub>/5% CO<sub>2</sub>) was used to determine if there was any SO<sub>4</sub><sup>2-</sup>/HCO<sub>3</sub><sup>-</sup> exchange. At the end of each experiment, pH<sub>i</sub> was calibrated using K<sup>+</sup> clamp solutions with 10 μmol/L nigericin (Cayman Chemical, Ann Arbor, MI) that were set at pH 6.8 and 7.6. The rate of initial alkalization after the switch from Cl<sup>-</sup> solution to Cl<sup>-</sup>-free solution was calculated using Origin 8.0 software (Origin-Lab, Northampton, MA).

### Determination of IC<sub>50</sub> of DRA Inhibitor

A novel small-molecule DRA inhibitor (DRA<sub>inh</sub>-A250) recently was developed by Dr Alan Verkman (University of California San Francisco, San Francisco, CA).<sup>20</sup> After exposure to the inhibitor in both apical and basolateral superfusate for at least 15 minutes, the effects of serial concentrations of the inhibitor (0, 0.1, 0.25, 0.5, 1, 2.5, and 5 μmol/L) on Cl<sup>-</sup>/HCO<sub>3</sub><sup>-</sup> exchange activity was studied. The IC<sub>50</sub> was calculated by a logistic regression model using Origin 8.0 software.

### Statistical Analysis

The results of at least 3 repeated experiments of HEK293 cells, Caco-2 cells, and colonoids were used for statistical analysis. Data are presented as means ± SEM. Statistical analyses were conducted using the Student *t* test or analysis of variance if more than 2 comparisons were performed. *P* < .05 was considered statistically significant.

## References

- Ghishan FK, Kiela PR. Small intestinal ion transport. *Curr Opin Gastroenterol* 2012;28:130–134.
- Singh AK, Riederer B, Chen M, Xiao F, Krabbenhöft A, Engelhardt R, Nylander O, Soleimani M, Seidler U. The switch of intestinal Slc26 exchangers from anion absorptive to HCO<sub>3</sub><sup>-</sup> secretory mode is dependent on CFTR anion channel function. *Am J Physiol Cell Physiol* 2010;298:C1057–C1065.
- Walker NM, Simpson JE, Brazill JM, Gill RK, Dudeja PK, Schweinfest CW, Clarke LL. Role of down-regulated in adenoma anion exchanger in HCO<sub>3</sub><sup>-</sup> secretion across murine duodenum. *Gastroenterology* 2009;136:893–901.
- Xiao F, Yu Q, Li J, Johansson ME, Singh AK, Xia W, Riederer B, Engelhardt R, Montrose M, Soleimani M, Tian DA, Xu G, Hansson GC, Seidler U. Slc26a3 deficiency is associated with loss of colonic HCO<sub>3</sub><sup>-</sup> secretion, absence of a firm mucus layer and barrier impairment in mice. *Acta Physiol (Oxf)* 2014;211:161–175.
- Gawenis LR, Hut H, Bot AG, Shull GE, de Jonge HR, Stien X, Miller ML, Clarke LL. Electroneutral sodium absorption and electrogenic anion secretion across murine small intestine are regulated in parallel. *Am J Physiol Gastrointest Liver Physiol* 2004;287:G1140–G1149.
- Gennari FJ, Weise WJ. Acid-base disturbances in gastrointestinal disease. *Clin J Am Soc Nephrol* 2008;3:1861–1868.
- Kato A, Romero MF. Regulation of electroneutral NaCl absorption by the small intestine. *Annu Rev Physiol* 2011;73:261–281.
- Sundaram U, Knickelbein RG, Dobbins JW. Mechanism of intestinal secretion: effect of cyclic AMP on rabbit ileal crypt and villus cells. *Proc Natl Acad Sci U S A* 1991;88:6249–6253.
- Ko SB, Shcheynikov N, Choi JY, Luo X, Ishibashi K, Thomas PJ, Kim JY, Kim KH, Lee MG, Naruse S, Muallem S. A molecular mechanism for aberrant CFTR-dependent HCO<sub>3</sub><sup>-</sup> transport in cystic fibrosis. *EMBO J* 2002;21:5662–5672.
- Chernova MN, Jiang L, Shmukler BE, Schweinfest CW, Blanco P, Freedman SD, Stewart AK, Alper SL. Acute regulation of the SLC26A3 congenital chloride diarrhoea anion exchanger (DRA) expressed in *Xenopus* oocytes. *J Physiol* 2003;549:3–19.
- Musch MW, Arvans DL, Wu GD, Chang EB. Functional coupling of the downregulated in adenoma Cl<sup>-</sup>/base exchanger DRA and the apical Na<sup>+</sup>/H<sup>+</sup> exchangers NHE2 and NHE3. *Am J Physiol Gastrointest Liver Physiol* 2009;296:G202–G210.
- Dunk CR, Brown CD, Turnberg LA. Stimulation of HCO<sub>3</sub><sup>-</sup>/Cl<sup>-</sup> exchange in rat duodenal brush border membrane vesicles by cAMP. *Pflugers Arch* 1989;414:701–705.
- Furukawa O, Bi LC, Guth PH, Engel E, Hirokawa M, Kaunitz JD. NHE3 inhibition activates duodenal bicarbonate secretion in the rat. *Am J Physiol Gastrointest Liver Physiol* 2004;286:G102–G109.
- Walker NM, Simpson JE, Yen PF, Gill RK, Rigsby EV, Brazill JM, Dudeja PK, Schweinfest CW, Clarke LL. Down-regulated in adenoma Cl<sup>-</sup>/HCO<sub>3</sub><sup>-</sup> exchanger couples with Na<sup>+</sup>/H<sup>+</sup> exchanger 3 for NaCl absorption in murine small intestine. *Gastroenterology* 2008;135:1645–1653 e3.
- Chang E, Rao M. Intestinal water and electrolyte transport: mechanisms of physiological and adaptive responses. In: LR J, ed. *Physiology of the gastrointestinal tract*. New York: Raven Press, 1994: 2027–2081.



16. Sellin JH, DeSoignie R. Rabbit proximal colon: a distinct transport epithelium. *Am J Physiol* 1984; 246:G603–G610.
17. In J, Foulke-Abel J, Zachos NC, Hansen AM, Kaper JB, Bernstein HD, Halushka M, Blutt S, Estes MK, Donowitz M, Kovbasnjuk O. Enterohemorrhagic reduce mucus and intermicrovillar bridges in human stem cell-derived colonoids. *Cell Mol Gastroenterol Hepatol* 2016;2:48–62 e3.
18. Yin J, Tse CM, Avula LR, Singh V, Foulke-Abel J, de Jonge HR, Donowitz M. Molecular basis and differentiation-associated alterations of anion secretion in human duodenal enteroid monolayers. *Cell Mol Gastroenterol Hepatol* 2018;5:591–609.
19. Simpson JE, Schweinfest CW, Shull GE, Gawenis LR, Walker NM, Boyle KT, Soleimani M, Clarke LL. PAT-1 (Slc26a6) is the predominant apical membrane  $\text{Cl}^-/\text{HCO}_3^-$  exchanger in the upper villous epithelium of the murine duodenum. *Am J Physiol Gastrointest Liver Physiol* 2007;292:G1079–G1088.
20. Haggie PM, Cil O, Lee S, Tan JA, Rivera AA, Phuan PW, Verkman AS. SLC26A3 inhibitor identified in small molecule screen blocks colonic fluid absorption and reduces constipation. *JCI Insight* 2018;3.
21. Domingue JC, Ao M, Sarathy J, George A, Alrefai WA, Nelson DJ, Rao MC. HEK-293 cells expressing the cystic fibrosis transmembrane conductance regulator (CFTR): a model for studying regulation of  $\text{Cl}^-$  transport. *Physiol Rep* 2014;2:e12158.
22. Park HW, Nam JH, Kim JY, Namkung W, Yoon JS, Lee JS, Kim KS, Venglovecz V, Gray MA, Kim KH, Lee MG. Dynamic regulation of CFTR bicarbonate permeability by  $[\text{Cl}^-]_i$  and its role in pancreatic bicarbonate secretion. *Gastroenterology* 2010;139:620–631.
23. Jacob P, Rossmann H, Lamprecht G, Kretz A, Neff C, Lin-Wu E, Gregor M, Groneberg DA, Kere J, Seidler U. Down-regulated in adenoma mediates apical  $\text{Cl}^-/\text{HCO}_3^-$  exchange in rabbit, rat, and human duodenum. *Gastroenterology* 2002;122:709–724.
24. Li J, Xia F, Reithmeier RA. N-glycosylation and topology of the human SLC26 family of anion transport membrane proteins. *Am J Physiol Cell Physiol* 2014; 306:C943–C960.
25. Hayashi H, Yamashita Y. Role of N-glycosylation in cell surface expression and protection against proteolysis of the intestinal anion exchanger SLC26A3. *Am J Physiol Cell Physiol* 2012;302:C781–C795.
26. Cordat E, Reithmeier RA. Structure, function, and trafficking of SLC4 and SLC26 anion transporters. *Curr Top Membr* 2014;73:1–67.
27. Kumar A, Chatterjee I, Gujral T, Alakkam A, Coffing H, Anbazhagan AN, Borthakur A, Saksena S, Gill RK, Alrefai WA, Dudeja PK. Activation of nuclear factor-kappaB by tumor necrosis factor in intestinal epithelial cells and mouse intestinal epithelia reduces expression of the chloride transporter SLC26A3. *Gastroenterology* 2017;153:1338–1350 e3.
28. Alper SL, Stewart AK, Vandorpe DH, Clark JS, Horack RZ, Simpson JE, Walker NM, Clarke LL. Native and recombinant Slc26a3 (downregulated in adenoma, Dra) do not exhibit properties of  $2\text{Cl}^-/\text{HCO}_3^-$  exchange. *Am J Physiol Cell Physiol* 2011;300:C276–C286.
29. Lamprecht G, Baisch S, Schoenleber E, Gregor M. Transport properties of the human intestinal anion exchanger DRA (down-regulated in adenoma) in transfected HEK293 cells. *Pflugers Arch* 2005; 449:479–490.
30. Marchelletta RR, Gareau MG, McCole DF, Okamoto S, Roel E, Klinkenberg R, Guiney DG, Fierer J, Barrett KE. Altered expression and localization of ion transporters contribute to diarrhea in mice with Salmonella-induced enteritis. *Gastroenterology* 2013; 145:1358–1368 e1–4.
31. Gill RK, Borthakur A, Hodges K, Turner JR, Clayburgh DR, Saksena S, Zaheer A, Ramaswamy K, Hecht G, Dudeja PK. Mechanism underlying inhibition of intestinal apical  $\text{Cl}^-/\text{OH}^-$  exchange following infection with enteropathogenic *E. coli*. *J Clin Invest* 2007; 117:428–437.
32. Xiao F, Li J, Singh AK, Riederer B, Wang J, Sultan A, Park H, Lee MG, Lamprecht G, Scholte BJ, De Jonge HR, Seidler U. Rescue of epithelial  $\text{HCO}_3^-$  secretion in murine intestine by apical membrane expression of the cystic fibrosis transmembrane conductance regulator mutant F508del. *J Physiol* 2012; 590:5317–5334.
33. Gentzsch M, Dang H, Dang Y, Garcia-Caballero A, Suchindran H, Boucher RC, Stutts MJ. The cystic fibrosis transmembrane conductance regulator impedes proteolytic stimulation of the epithelial  $\text{Na}^+$  channel. *J Biol Chem* 2010;285:32227–32232.
34. Huang J, Kim D, Shan J, Abu-Arish A, Luo Y, Hanrahan JW. Most bicarbonate secretion by Calu-3 cells is mediated by CFTR and independent of pendrin. *Physiol Rep* 2018;6.
35. Ko SB, Zeng W, Dorwart MR, Luo X, Kim KH, Millen L, Goto H, Naruse S, Soyombo A, Thomas PJ, Muallem S. Gating of CFTR by the STAS domain of SLC26 transporters. *Nat Cell Biol* 2004;6:343–350.
36. Foulke-Abel J, In J, Yin J, Zachos NC, Kovbasnjuk O, Estes MK, de Jonge H, Donowitz M. Human enteroids as a model of upper small intestinal ion transport physiology and pathophysiology. *Gastroenterology* 2016; 150:638–649.e8.
37. Singh V, Lin R, Yang J, Cha B, Sarker R, Tse CM, Donowitz M. AKT and GSK-3 are necessary for direct ezrin binding to NHE3 as part of a C-terminal stimulatory complex. *J Biol Chem* 2014;289:5449–5461.
38. Sarker R, Valkhoff VE, Zachos NC, Lin R, Cha B, Chen TE, Guggino S, Zizak M, de Jonge H, Hogema B, Donowitz M. NHERF1 and NHERF2 are necessary for multiple but usually separate aspects of basal and acute regulation of NHE3 activity. *Am J Physiol Cell Physiol* 2011;300:C771–C782.

---

Received August 20, 2018. Accepted January 7, 2019.

#### Correspondence

Address correspondence to: Mark Donowitz, MD, Johns Hopkins University School of Medicine, 925 Ross Research Building, 720 Rutland Avenue, Baltimore, Maryland 21205. e-mail: mdonowitz@jhmi.edu; fax: (410) 955-9677.

**Acknowledgments**

The authors would like to thank Dr Liudmila Cebotaru (Johns Hopkins University, Baltimore, MD) for providing the GFP-CFTR construct and Ardelyx, Inc (Fremont, CA) for providing Tenapanor.

**Author contributions**

Chung-Ming Tse was responsible for the study concept and design, acquisition of data, analysis of data, and drafting the manuscript; Jianyi Yin was responsible for the study concept and design, acquisition of data, analysis of data, and drafting the manuscript; Varsha Singh, Rafiquel Sarker, and Ruxian Lin acquired and analyzed data; Alan S. Verkman provided material support and obtained funding; Jerrold R. Turner acquired data and

obtained funding; and Mark Donowitz was responsible for the study concept and design, acquisition of data, analysis of data, drafting of the manuscript, and obtained funding.

**Conflicts of interest**

The authors disclose no conflicts.

**Funding**

This study was supported in part by National Institutes of Health grants R01-DK-26523 (M.D.), R01-DK-61765 (M.D.), P01-DK-072084 (M.D.), R24-DK-64388 (M.D.), U18-TR000552, UH3-TR00003 (M.D.), U01-DK-10316 (M.D.), and P30-DK-89502 (M.D.).